SPARC-MM-05/002
20 September 2005

THE SPARC STEERING MAGNETS:

MEASUREMENTS ON THE ACCELERATING SECTION STEERING PROTOTYPE

B. Bolli, S. Ceravolo, F. Iungo, C. Ligi, M. Paris, M. Preger,
C. Sanelli, F. Sardone, F. Sgamma, M. Troiani,
G. Bazzano, D. Bianculli*, I. De Cesaris**

INFN-LNF
**Fondazione CNAO*

Abstract

The electrical and magnetic measurements made on the sections steering magnet prototype for SPARC, in comparison with the results of the 3D simulations, are reported.

1. Introduction

Several steering magnets are foreseen along the SPARC beam line. All these magnets consist of *cos(θ)*–like coils, where the copper conductor is wounded on an aluminium support. No ferromagnetic materials must be used.

7 couples of horizontal plus vertical steering magnets, one inside the other, will surround 7 Beam Position Monitor (BPM steerings), while 6 other couples will surround 3 accelerating sections of SPARC (section steerings). The prototype of the BPM steerings is under construction and will be described in another Technical Note. Here we describe the magnets that are planned to be installed around the accelerating sections. Each magnet will deflect the beam in only one direction. They will be organized in 6 couples near the beginning and the end of the 3 accelerating sections. The accelerator layout is shown in Figure 1. Each arrow indicates the position of a couple of vertical plus horizontal steering magnets.

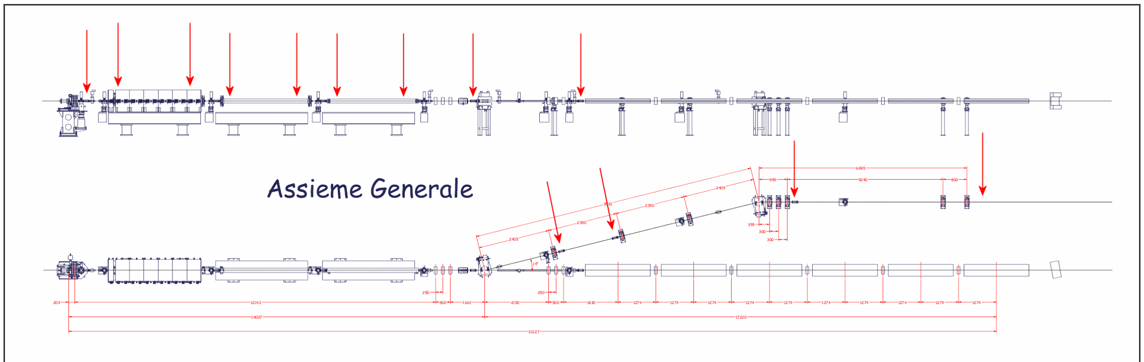

Figure 1: The SPARC layout

Every couple of the "Accelerating Section" steerings (see Figure 2) is made of 2 identical magnets, one near the other, the second rotated by 90 degrees with respect to the first one, in order to accomplish an independent horizontal or vertical steering of the beam (see Figure 3). They will be mounted directly around the accelerating sections (of cylindrical shape) by means of screws.

The magnet has been designed following the so-called *cos(θ)* current distribution, without ferromagnetic yoke, in order to obtain a very compact solution. Table I lists the main parameters. The magnetic simulations were made by means of the 3D code OPERA.

A prototype of the section steering magnets has been built and measured to verify the magnetic simulations.

Tab. I – *Section Steering Magnet prototype design parameters*

Cos(θ) Steering H/V	**Units**	**Value**
Energy (max)	MeV	230
Deflection angle (max)	mrad	0.75 (@ 230 MeV)
Copper Wire Diameter	mm	3
Magnet Radius	mm	80.5
Magnetic Length	mm	108
Maximum Current	A	30
Field @ Max. Current	Gauss	45.1
Field Homogeneity	$\Delta B/B$ @ ±10 mm	$1.6*10^{-3}$

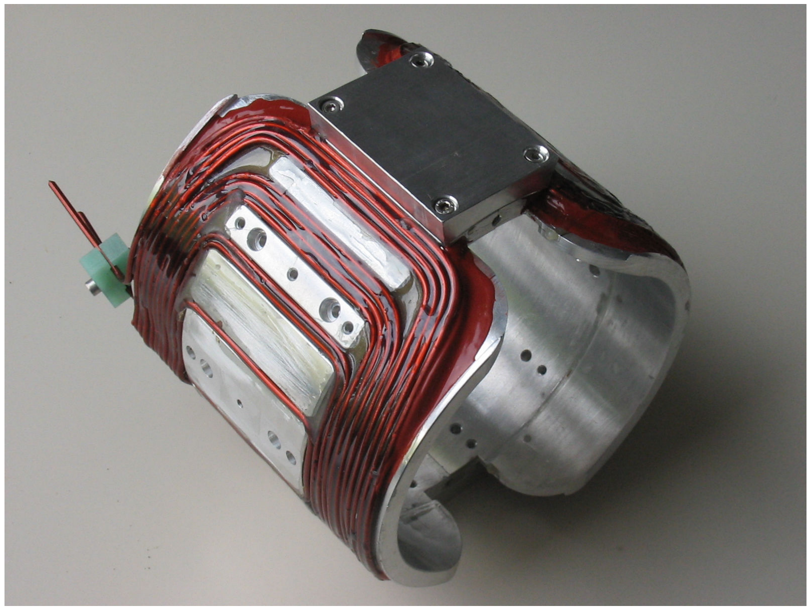

Figure 2: The section steering magnet prototype

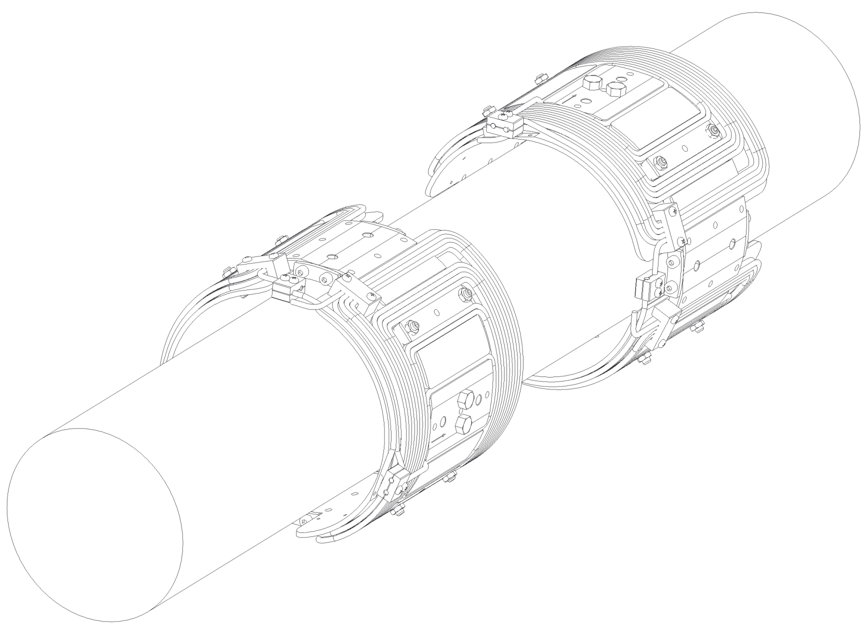

Figure 3: Sketch of a couple of Section Steering Magnets surrounding the accelerating section

2. Electrical Measurements

The resistance of the magnet was measured by means of the Volt-Ampere method at room temperature using the following instrumentation:

Power supply: FUG NLB 700-20
Voltmeter: Fluke mod. 77

The following values were measured at Tamb = 22.5 °C:

$\Delta V = 0.255$ V @ $I = 5$ A
$\Delta V = 1.530$ V @ $I = 30$ A

corresponding to a DC resistance of 0.051 Ω.

The inductance and resistance of the steering magnet was also measured by means of a LCR meter, HP mod. 4284 A, at different frequencies. Results are shown in Figure 4. The corresponding DC values can be extrapolated from these data. Table II lists the measured values. They are consistent with the design data.

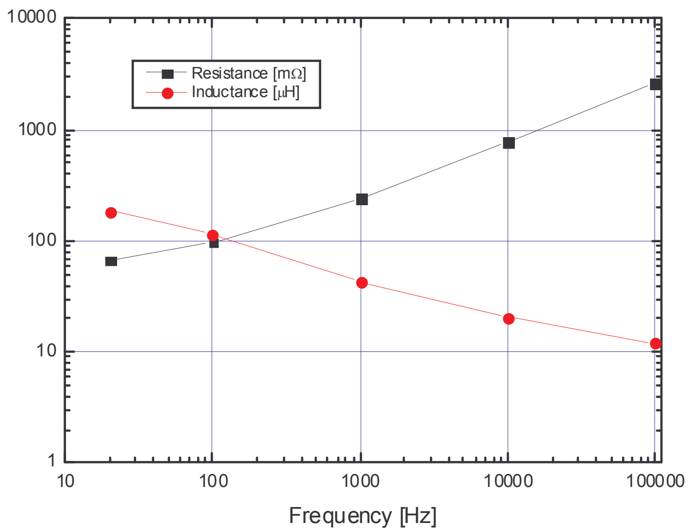

Figure 4: Steering magnet Resistance and Inductance versus frequency

Table II – *Resistance and Inductance versus frequency.*

Frequency (Hz)	R (mΩ)	L (μH)
20	66.6	185.6
100	97.6	116.3
1 k	239.8	43.07
10 k	779	20.7
100 k	2626	11.9

Figure 5 and Figure 6 show the temperature increase on the coil and the Aluminum support respectively together with the best fit curve on the experimental data. The room temperature was ≈ 23 °C. Measurements are in good agreement with an expectation of ΔT ≈ 29 °C

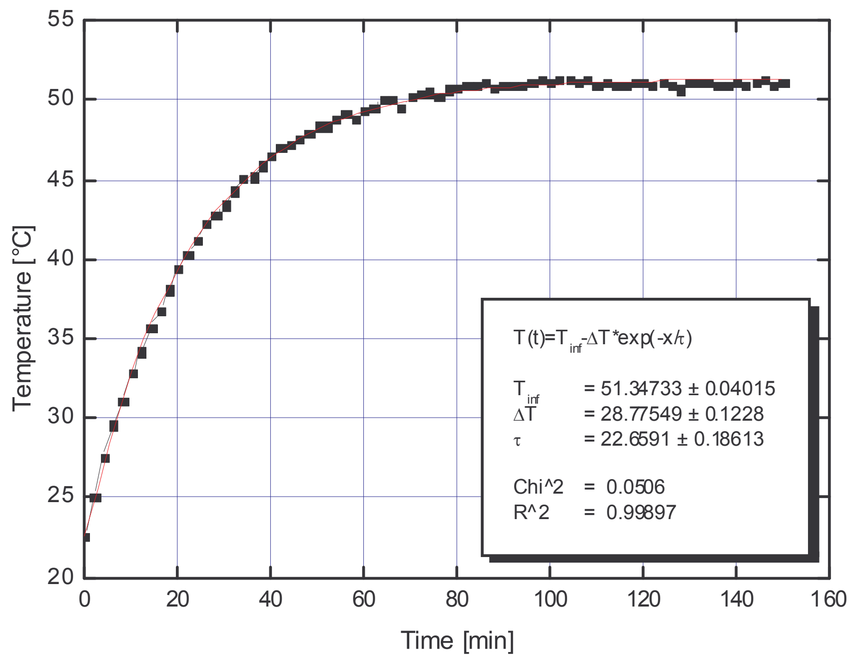

Figure 5: Temperature increase on the coil

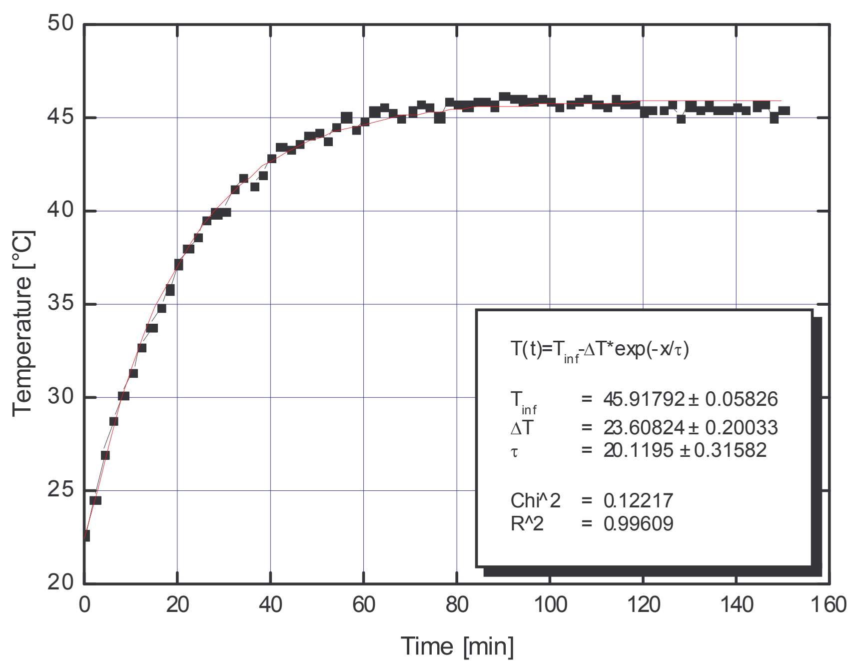

Figure 6: Temperature increase on the aluminum support

3. Magnetic Measurements

All the measurements have been taken with the magnet configured as a vertical corrector, therefore only the horizontal component of the field is considered. In the following, *z* is the vertical, *y* the longitudinal (the beam direction) and *x* the horizontal coordinate.

A new Hall probe with a resolution of 10^{-3} Gauss has been used.

The horizontal component of the earth magnetic field has been measured to be -0.3 Gauss. This component has not been subtracted from the measured values reported in this paper.

Figure 7 and Figure 8 show two outputs of the OPERA 3D simulations. They show the amplitude of the horizontal component of the field B_x (colors) and the direction of the total field B (vectors) in the *x-z* and in the *x-y* plane respectively. Due to the absence of any ferromagnetic material, only the magnet coils have been considered in the simulations.

Figure 9 shows the measured B_x at the magnet centre as function of the current. Since the power supply is bipolar, the current values span from -30A to +30A. Since there is no iron, the field-current curve is absolutely linear. The earth magnetic field, at zero current, gives a negligible offset. The measurement confirms the design expectations.

The behaviour of the field has been measured in steps of 10 mm along straight lines parallel to the magnet axis, at horizontal and vertical distances from it with steps of 10 mm (5mm for the vertical ones in the good field region). We remind that the requested good field is within ± 10 mm (see table I), but the measurements have been extended till ± 30 mm.

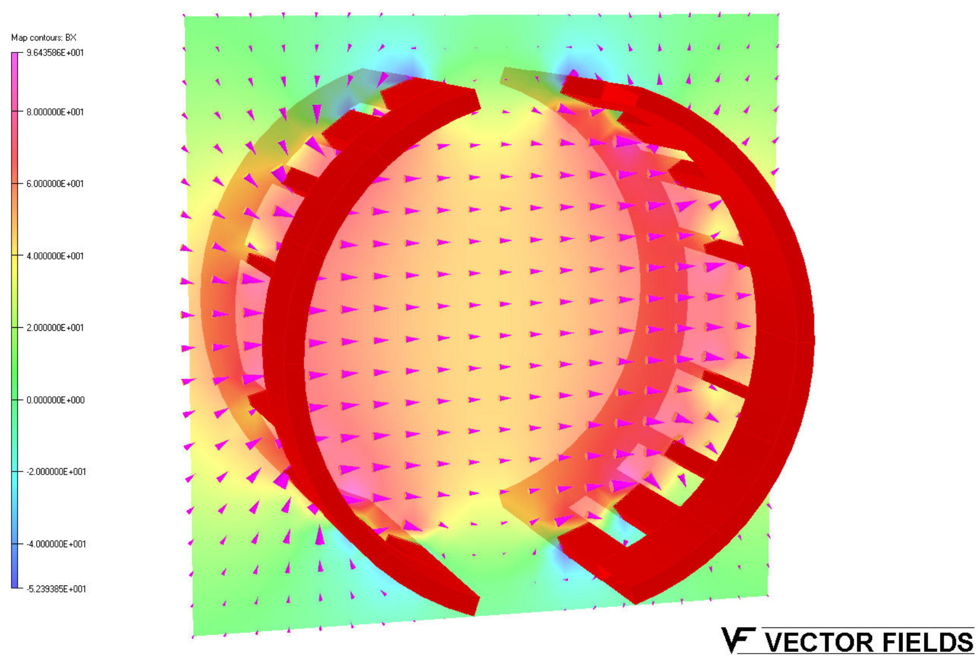

Figure 7: OPERA-3D simulation of the magnetic field in the vertical plane at magnet centre

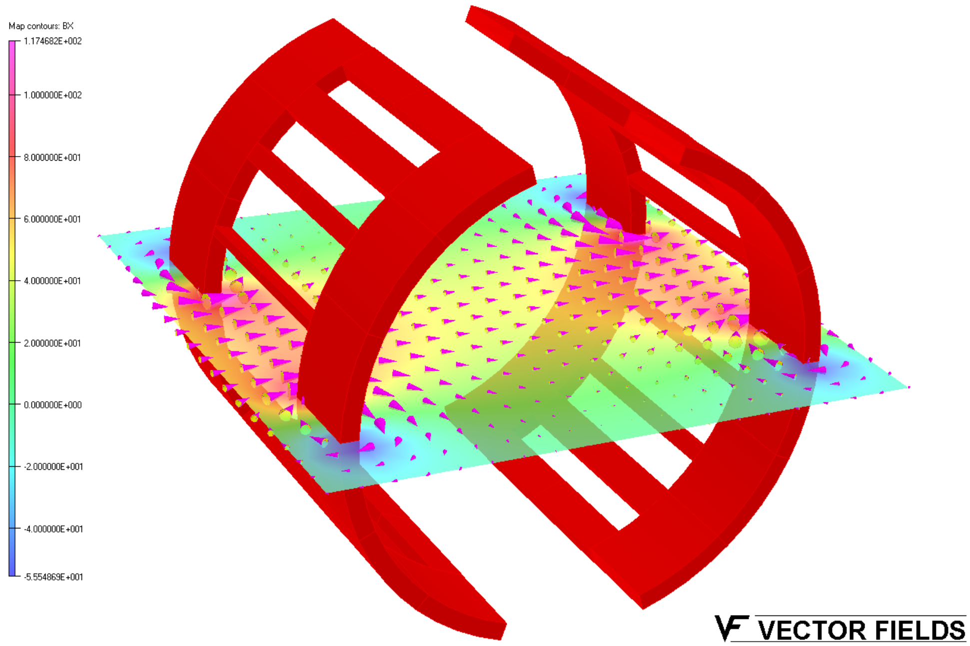

Figure 8: OPERA-3D simulation of the magnetic field in the horizontal plane at magnet centre

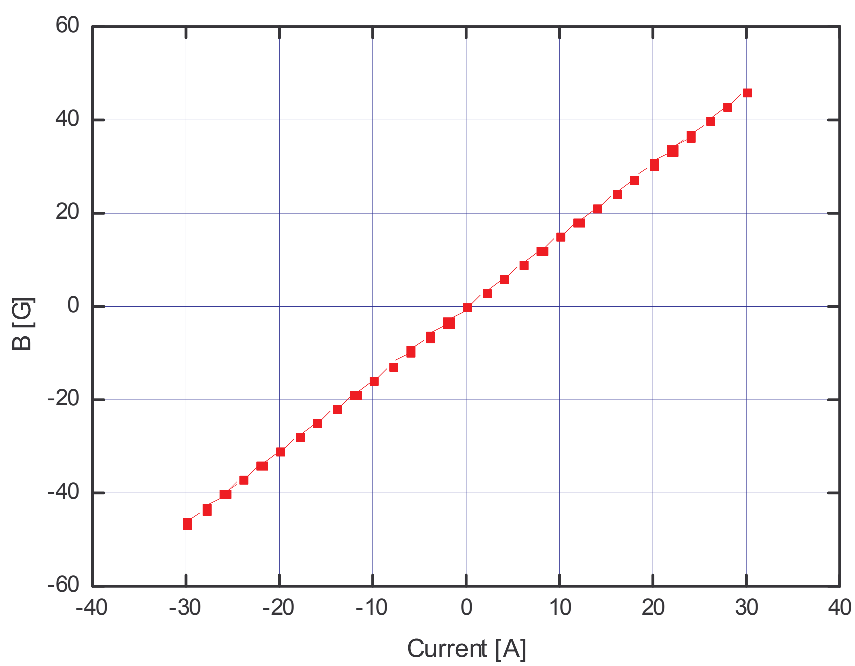

Figure 9: Horizontal component of the magnetic field at the magnet centre versus current

The measured field values are in quite good agreement with those obtained simulating the steering magnet by means of the 3D code OPERA. Figure 10 shows the measured and calculated horizontal component of the field versus vertical positions at magnet centre at the maximum current value (30 A). The measured value is 1.8 % higher than the expected, and the field quality inside the good field region (±10 mm) is $\Delta B/B = 1.9\ 10^{-3}$ versus a calculated value of 1.6 10^{-3}. Figure 11 shows the measured B_x versus the z coordinate at different x positions. There is a small right-left asymmetry in the measured data, but it becomes significantly only far from the central axis.

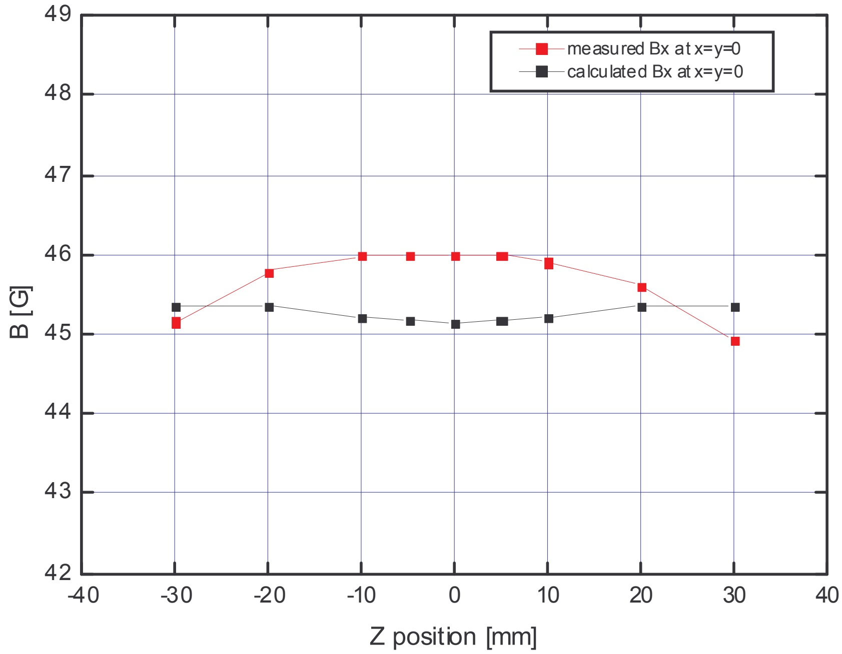

Figure 10: Measured (red) and calculated (black) horizontal component of the field at the magnet center versus the vertical position @ 30 A

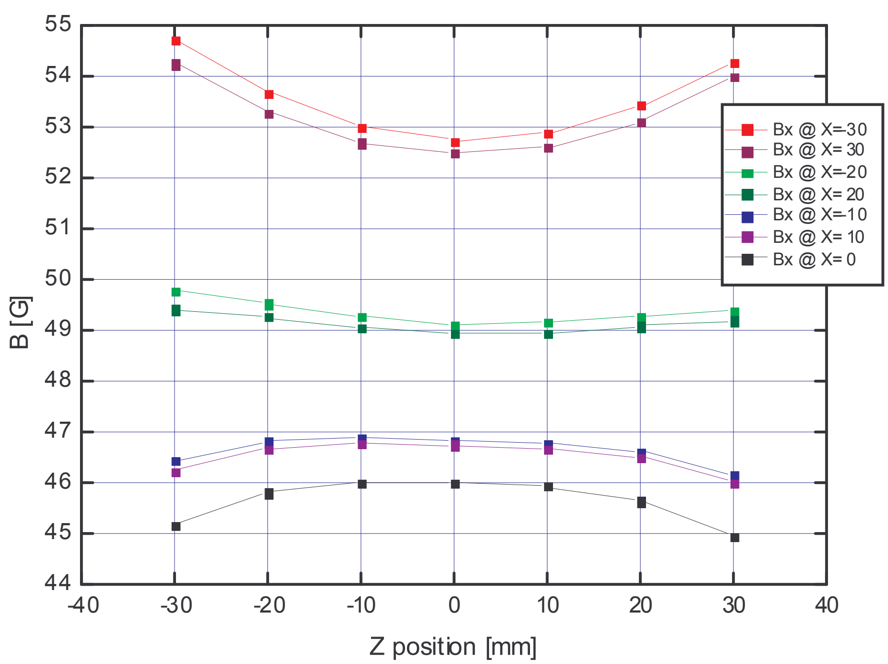

Figure 11: Measured horizontal component of the field at y = 0 versus the vertical position @ 30 A for different horizontal positions

Figure 12 shows the comparison between the measured and calculated horizontal component of the field along the magnet axis, while the measured field at different horizontal positions is given in Figure 13. The full width at half maximum is 120.8 mm. From Figure 12 a small shift of ≈ 1.8mm between the two curves can be noticed.

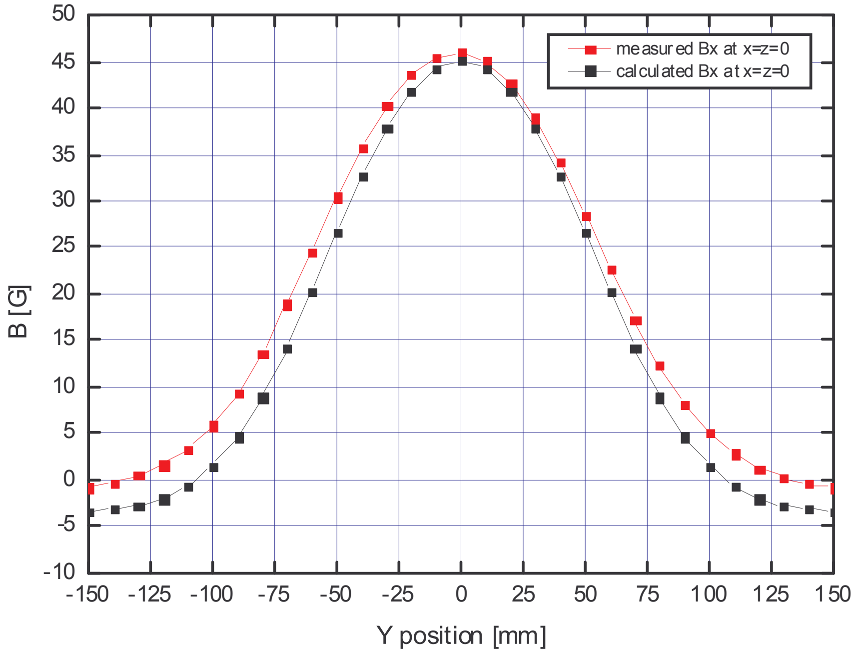

Figure 12: Measured (red) and calculated (black) horizontal component of the field at the magnet center versus the longitudinal position @ 30 A

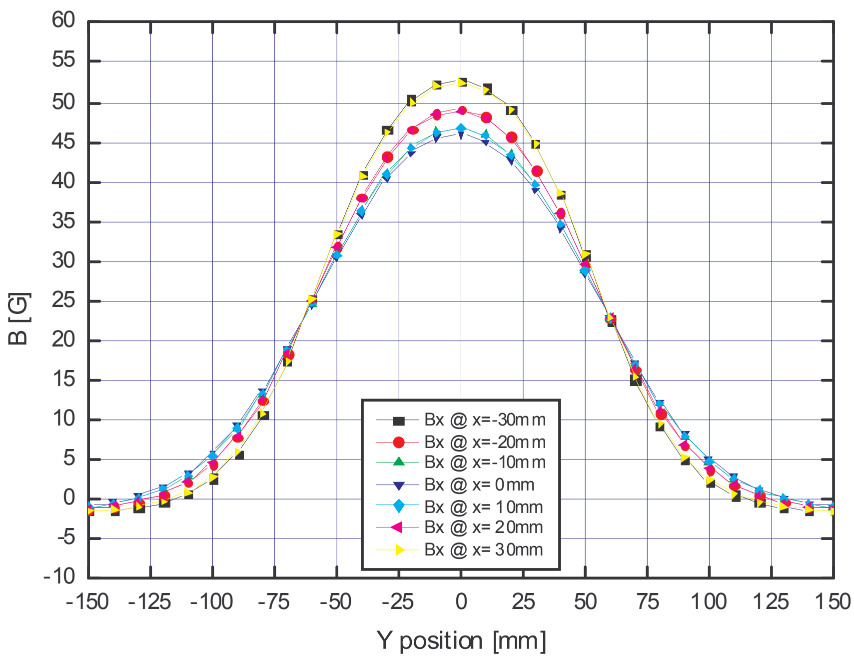

Figure 13: Measured horizontal component of the field at z = 0 versus the longitudinal position @ 30 A for different horizontal positions

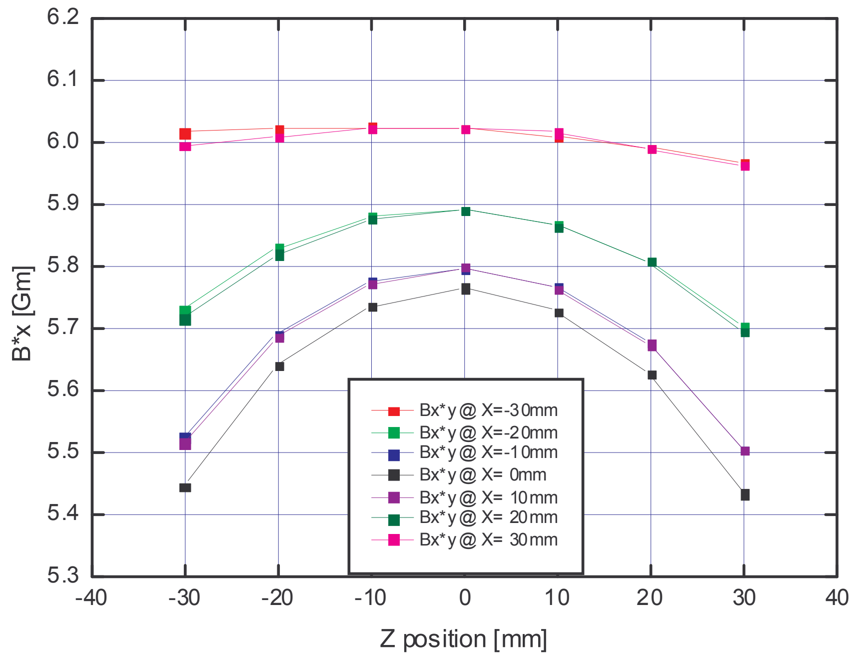

Figure 14: Integrated horizontal component of the field versus the vertical position @ 30 A for different horizontal positions

$\int B_x dy$ between ±150 mm from the centre is given in Figure 14 for different x positions.

The measured magnetic length is 124mm. However, it must be observed that there are long tails and it must be kept in mind that when installed near other magnetic elements, the calibration can change significantly due to the absorption of the field lines by the yokes of the neighbouring magnets. In particular, the field of the steering magnets positioned around the first accelerating section will be affected by the presence of the iron of the big solenoid of SPARC. Simulations show that the iron should increase the field amplitude, without modifying significantly the shape of the field distribution and therefore the field quality.

Thanks to the linearity of the field versus current (Figure 9), taking the average value of the integrated horizontal field component measured in the good field region, the angular kick α can be expressed as a function of the beam energy and the excitation current as:

$$\alpha \text{ (mrad)} = 5.77 * 10^{-3} * \text{I (A)/E(GeV)}.$$

4. Conclusions

The SPARC section steering magnet prototype has been fully characterised, and the measurements confirmed the reliability of its magnetic design. The quality of the field is in good agreement with the simulations, the peak and integrated values being slightly larger than expected.

The linearity of the magnetic field with the excitation current makes the overall orbit correction procedure easier.

The interference of the field tails with the yoke of other magnetic components must be kept in mind and carefully checked during commissioning by calibrating the steering magnet with the beam itself.